



OTC 17535

## Structural Reliability Applications in Risk-Based Inspection Plans and Their Sensitivities to Different Environmental Conditions

A.P. Ku and R.E. Spong, Energo Engineering; C. Serratella, ABS Consulting, Inc.; X.S. Wu, ExxonMobil Upstream Research Company; and R. Basu and G. Wang, American Bureau of Shipping

Copyright 2005, Offshore Technology Conference

This paper was prepared for presentation at the 2005 Offshore Technology Conference held in Houston, TX, U.S.A., 2-5 May 2005.

This paper was selected for presentation by an OTC Program Committee following review of information contained in a proposal submitted by the author(s). Contents of the paper, as presented, have not been reviewed by the Offshore Technology Conference and are subject to correction by the author(s). The material, as presented, does not necessarily reflect any position of the Offshore Technology Conference, its officers, or members. Papers presented at OTC are subject to publication review by Sponsor Society Committees of the Offshore Technology Conference. Electronic reproduction, distribution, or storage of any part of this paper for commercial purposes without the written consent of the Offshore Technology Conference is prohibited. Permission to reproduce in print is restricted to a proposal of not more than 300 words; illustrations may not be copied. The proposal must contain conspicuous acknowledgment of where and by whom the paper was presented. Write Librarian, OTC, P.O. Box 833836, Richardson, TX 75083-3836, U.S.A., fax 01-972-952-9435.

### Abstract

Structural system inspection practices for floating offshore facilities, such as FPSO's and FSO's, have for the most part followed the practice employed and developed via trading ships/maritime practice. Often, the influence of a particular repeated service/cargo loading regime, cargo corrosivity, or site environmental influence can play a major role for a particular asset. More specifically, there has been only cursory attempts made to first understand and then, where possible, take advantage of site-specific conditions and loading in the development of in-service inspection plans.

In recent years there has been significant interest by the marine and offshore industry to apply structural reliability techniques to risk based inspection planning for marine vessels and floating production installations. In this regard, structural reliability based methods can assist in providing a framework for quantifying site-specific loading and degradation mechanisms (such as fatigue and corrosion), through a systematic consideration of the probabilistic uncertainty in each degradation mechanism. By applying structural reliability analysis and risk assessment techniques to inspection planning, the operator is given a tool by which he can justify the allocation of resources to those structural components with a higher risk profile, and at the same time potentially relax inspection activities for low risk components to optimize and target inspection efforts.

In a companion paper [1], available structural reliability methods developed to date were summarized, and then applied to determine the inspection intervals based on site specific loading as applied to strength considerations of the hull girder as well as to stiffened and un-stiffened plate panels. By tracing the time-varying reliability index for these structural components, the risk-based inspection intervals can be determined. This methodology has recently been

implemented to provide the foundation in a risk-based inspection (RBI) plan for a floating production unit offshore West Africa. The current paper will further consider the sensitivities resulting from the following two conditions for the strength reliability: (1) environmental load for different regions of the world, and (2) corrosion rate corresponds to offshore environment as well as storage conditions. Another two conditions are considered for fatigue reliability: (3) assumed initial crack size for a connection, and (4) crack growth parameter for either the air environment or marine environment that a connection may be subjected to. The sensitivity studies presented in this paper provide a quick reference to understand the RBI plans benefits via work scope optimization and cost reductions for floating production units operating in various regions of the world.

### Introduction

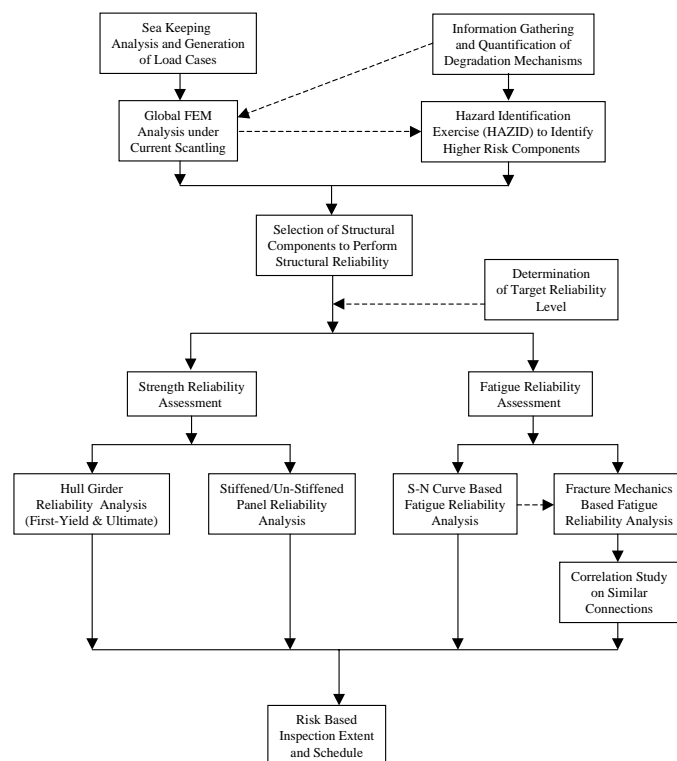


Figure 1 - A risk-based inspection planning reliability analysis flow chart [1]

Details of a structural reliability methodology applicable to risk based inspections on a ship-shaped floating production vessel have been published in a companion paper [1]. From that paper, a flow chart of this methodology is shown in Figure 1. This methodology starts with information gathering, such as obtaining the vessel gauging data, vessel past history, current service condition, etc.

For the example vessel considered in [1], direct sea-keeping and global finite element analysis were conducted to identify representative high-stressed structural components of all types for further structural reliability analyses. The model plot of this global finite element analysis is shown in Figure 2.

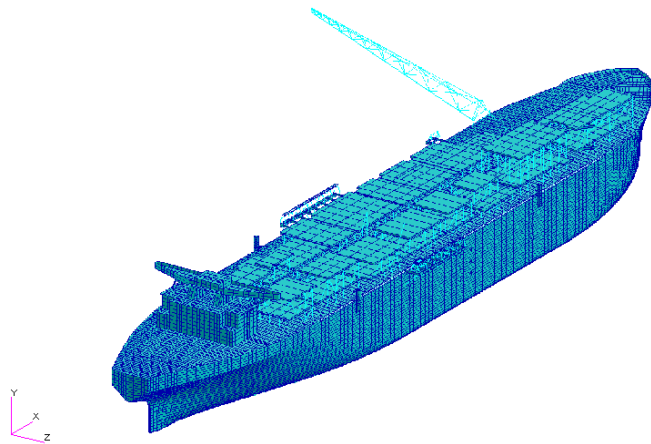


Figure 2 - Global FEM model of an example FPSO [1]

The strength reliability analyses were carried out both on the global strength level and local strength level. For global strength analysis, several frames along the length of the vessel were selected and their first-yield strength as well as the ultimate strength was analyzed. Corrosion rates and the wave-induced bending moment were considered as random variables, among others, for the global strength analysis.

For local strength analysis, a representative number of plate panels were selected with the objective to envelope the load and expected corrosion conditions along the entire length of the vessel. Similar to the hull girder strength analysis, the primary stress component due to wave-induced motion, together with corrosion rates applicable to the plate and stiffeners, were considered as the main random variables.

The strength reliabilities for both the hull girder and plate panels were calculated on an annual basis and compared to a chosen target value to determine if the reliability values (reliability index) are acceptable. The target values were determined from a risk diagram as shown in Figure 3.

Figure 3 combines the consequence and likelihood information on one chart, which also conveniently overlay the experiences from other industries such that the current application can be put into perspective. The highest consequence (Consequence I) implies the total loss of vessel plus the loss of production for a time period of approximately two years. Consequence II is one order of magnitude less (i.e., represents significant damage) than Consequence I in terms of financial loss, and similarly for Consequence III.

The target reliabilities are also compared to the published Ship Structure Committee recommended values for tankers [2], which is presented in Table 1. Note that in Table 1, Consequence I is further divided into I-a and I-b, in which Consequence I-a applies to reliability analysis if the hull girder first-yield capacity is considered. Consequence I-b applies to hull girder ultimate capacity analysis. Since first-yield capacity typically overestimates the true capacity of the hull girder, a higher reliability level is required. The Consequence I as shown in Figure 3 is for Consequence I-b for the ultimate capacity, which represents the true capacity of the hull girder.

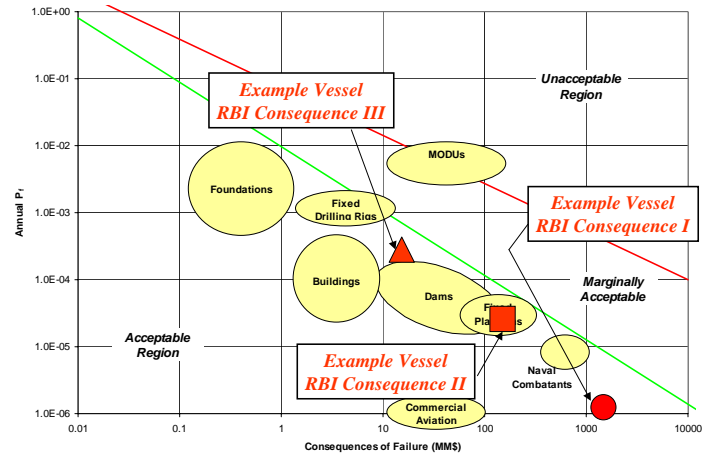


Figure 3 - Risk diagram to determine acceptable annual probability for various financial consequences [1]

Table 1 - Lifetime target reliability comparison between example vessel and Ship Structure Committee report [2] recommended values

Consequence	Strength Assessment		Fatigue Assessment	
	Example Vessel	Ship Structure Committee	Example Vessel	Ship Structure Committee
I-a	4.50	4.50	N/A	N/A
I-b	4.00	4.00	N/A	N/A
II	3.20	3.50	3.20	3.00
III	2.50	3.00	2.50	2.50
IV	1.50	N/A	1.50	2.00

Note: I-a refers to hull girder first-yield reliability  
I-b refers to hull girder ultimate reliability

In summary, the consequence levels (i.e., I-a, I-b, II, III and IV) are associated with the lifetime target reliabilities such that specific structural damage (i.e., fatigue or strength) should not drop below the assigned target probability.

**Part I: Strength Reliability Sensitivity**

This section focuses on the strength reliability of an example plate panel in a ship-shaped production vessel. The plate panel considered is a longitudinal bulkhead (LBH) plate located toward the bottom plating. This LBH plate is shown in Figure 4, which is subject to relatively high stress from hull girder bending moments. There are other relatively high stressed areas shown in Figure 4, for example toward the aft end of the LBH. However, stresses in this region are

dominated primarily from the geometry change and less so from the environmental loads.

The reliability limit state function of this LBH plate can be written as follows:

$$g = B_r \times R - B_s \times S \tag{1}$$

where  $R$  and  $S$  represent the probabilistic resistance and load variables.  $B_R$  and  $B_S$  are the model uncertainty factors for the resistance and load calculations, respectively. The details on the probabilistic distributions for  $B_R$  and  $B_S$  can be found in [1].

The resistance variable,  $R$ , is a set of plate buckling equations, the details of these equations can be found in Reference [3]. In these equations the main variables are the geometry of the plate panel, the number of stiffeners within the plate panel, and thickness of the plate and stiffeners. The corrosion rates have a direct impact on the plate and stiffener thickness and whose sensitivity will be studied in the following reliability analysis. The geometry of the plate panel is of the typical size found between two web frames encountered in a traditional VLCC tanker.

The load variable,  $S$ , consists of the wave-induced and still water induced bending moments. For simplicity, the still water-induced bending moment is treated as a fixed value among all sensitivity cases studied. The differences in load variable  $S$  are then primarily from wave environmental load and will be distinguished among four major offshore production regions of the world: West Africa, Brazil, Gulf of Mexico and North Sea in the following sensitivity study.

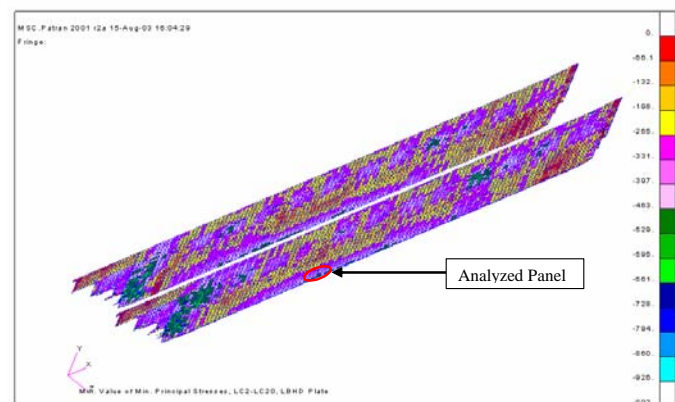


**Figure 4- A longitudinal bulkhead plate used for strength reliability sensitivity analysis**

**Environmental Load**

Reference [4] performed sea-keeping calculations to estimate the maximum vertical wave bending moment (VWBM) acting on the mid-section hull girder of a tanker-shaped floating vessel. The ratios between the maximum VWBM for four major offshore production regions of the world are shown in Table 2. Note that in Table 2 the ratios are normalized with respect to the West African (lowest) value.

**Table 2 – Ratio of Vertical Wave Bending Moment of a 315m Tanker Shaped Vessel**

West Africa	1.00
Brazil	1.27
GOM	1.40
North Sea	2.04

The primary stress component (longitudinal stress) on the LBH plate panel is assumed to be in direct proportion to the VWBM. In the reliability analysis the longitudinal stress is modeled as a Type-I extreme value distribution [1]. Also the distribution parameters of this distribution were calculated from direct sea-keeping analysis with West African wave conditions [1]. In the current reliability sensitivity study, the longitudinal stress distributions have mean values scaled by the ratios of Table 2, which the coefficient of variations are maintained the same for the four offshore regions considered.

**Corrosion Rate**

In addition to the four environmental cases, the influence of three representative corrosion rates (i.e., high, medium and low) are also evaluated in the study. The rate distributions are assumed to be represented by the Weibull distribution function. Table 3 shows the three assumed rates statistics (i.e., mean and coefficient of variation (c.o.v.)).

**Table 3 – Weibull Probabilistic Corrosion Rates Used for LBH Structural Elements**

	Mean (mm/year)	c.o.v.
Low Corrosion	0.08	50%
Medium Corrosion	0.16	50%
High Corrosion	0.30	50%

The mean rates shown in Table 3 are assumed for all of the structural elements (i.e., LBH plating, longitudinal webs and flanges). Furthermore the mean rate represents total material wastage for both sides of the structural element. This assumes that all elements, regardless of their orientation will have the same rate of material loss, and that both sides of the LBH plating is exposed to the same service conditions (i.e., crude oil storage tanks on both sides of LBH).

The three rates in Table 3 represent uniform corrosion for an uncoated surface exposed to crude oil. The low and medium corrosion are from the Guidance Manual for Tanker Structures [8] suggested corrosion rate range for LBH plating and longitudinal webs. The low corrosion represents the lower range rate, and medium corrosion represents upper range rate. The high corrosion is approximately twice that of the upper rates suggested in Reference 8, and it is intended to represent a severe general corrosion case.

For all rates, the c.o.v. is assumed to be 50%. Corresponding statistical values for oil tankers can be found in, e.g., [5]. In [5], and other accompanying references in [5], many thousands of gauging data from a wide range of tankers were analyzed with statistical distribution parameters calculated. The c.o.v. from those analyses is in the range of 100% for a wide range of structural components. However, the data was gathered from a wide spectrum of tankers,

potentially with very different tank service conditions and integrity management philosophies. In FPSO service for a single vessel, we expect the coefficient of variation to be smaller than the values given in [5].

Combining the four cases for environmental load conditions and three corrosion rate cases, there are a total of 12 cases considered in this strength reliability sensitivity study. These 12 cases are listed in Table 4 for easy reference.

**Table 4 – Case Number for Different Combinations of Environmental Load and Corrosion Rate**

	Low Corrosion	Medium Corrosion	High Corrosion
West Africa	1	2	3
Brazil	4	5	6
GOM	7	8	9
North Sea	10	11	12

### Strength Reliability Variations for Sensitivity Cases Considered

Figure 5 shows the strength reliability sensitivities for Cases 2, 5, 8 and 11 in which the corrosion rates were set to the medium level, with the environmental loads varied from West Africa to North Sea wave conditions.

Results from Figure 5 indicate that the example LBH plate panel has a sufficient reliability for almost the entire duration of design life (20 years) for West Africa, Brazil and GOM. In terms of scheduling of the risk based inspection interval, this plate panel and all other panels with smaller stress will not dominate the inspection interval. Also, the strength reliability is found to be not sensitive among these three environmental conditions.

The strength reliability for the North Sea environmental wave condition is found to be substantially lower than the other three environmental regions. A plate panel which might not dominate the RBI schedule consideration in the first three regions can become a dominant issue when the vessel is located in the North Sea.

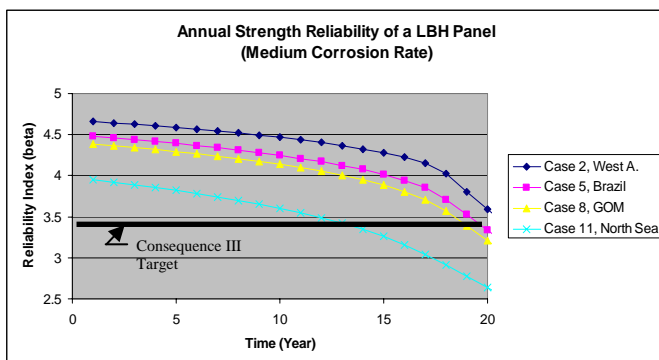


**Figure 5 – Annual Strength Reliability for Four Environmental Loads with Medium Corrosion Rate**

It needs to be pointed out that the target reliability level shown in Figure 5 is the annual target reliability, which is 3.4 for the Consequence III category. In Table 1 where the target reliabilities for various consequences are listed, the lifetime

target reliability values are used for the purpose of convenient comparison to [2].

Figure 6 shows the strength reliability sensitivities for Cases 7, 8 and 9 in which only the GOM environmental load is considered with the corrosion rates varied from low to high levels.

Results from Figure 6 show that the corrosion rates have major impacts on the strength reliability. For example, Case 7 (low corrosion rate) passes through the acceptable level at roughly year 50 (extrapolated beyond shown in Figure 6), while Case 8 (medium rate) passes through at year 18 and Case 9 (high rate) passes through at year 10.

Also as observed in Figure 6, the rate of strength reliability deterioration is very different for the three corrosion rate cases with the high corrosion rate case falling much more precipitately than the other two cases.

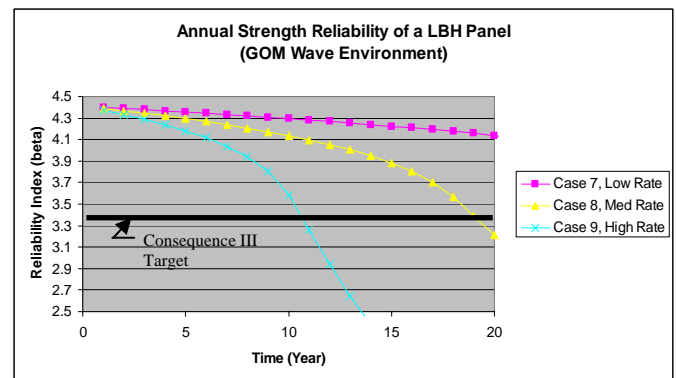


**Figure 6 – Annual Strength Reliability for Three Corrosion Rates with GOM Environmental Load**

It is found from the combined information given in Figures 5 and 6 that the RBI schedule has more sensitivity with respect to corrosion rate than to environmental load conditions. A vessel located in the North Sea can be kept with a high strength reliability level throughout the service life with lower corrosion rates, even though the environmental load is much more demanding compared to the other regions of the world.

Note that the effects of low corrosion rate uncertainty can be achieved in two independent ways: by lowering the expected (mean) corrosion rate or by lowering the spread (c.o.v.) of the corrosion uncertainty. For example, the same reliability can be achieved between a corrosion rate random variable with a mean value of 0.08 mm/year with a 50% c.o.v. and another corrosion rate with mean value of 0.3 mm/year but a smaller c.o.v. (e.g. 20%). This implies that even for vessels with high expected rates, due to anticipated tank service conditions (e.g., high cargo temperatures, infrequent tank usage, etc.), high reliability can still be achieved by implementing methods to closely monitor the corrosion rates observed in order to reduce the uncertainty associated with this high rate.

## Part II: Fatigue Reliability Sensitivity

In this section, the fatigue reliability sensitivity with respect to different initial crack sizes and crack growth parameters are examined. Figure 7 illustrates surface cracks propagated from a weld toe. Fatigue reliabilities were

calculated using fracture mechanics formulation, with the failure criterion defined as a through-thickness crack.

The development of fracture mechanics based fatigue reliability equations can be found in, e.g., [1], [6]. The limit state function reads:

$$M_i(t) = \int_{a_{oi}}^{a_{di}} \frac{da}{\left(\varepsilon_y Y(a) \sqrt{\pi a}\right)^m} - C_i \left( v_2 T \cdot \varepsilon_{s2}^m A^m \Gamma\left(1 + \frac{m}{B}\right) \right) \quad (2)$$

where

- $a_{oi}$  is the initial crack depth,
- $a_{di}$  is the final crack depth at fatigue failure,
- $Y(a)$  is the geometry function of the crack shape,
- $C_i, m$  are the crack growth parameters of the material,
- $v_2$  is the stress range annual frequency (cycles/year),
- $T$  is the time under consideration (year),
- $\varepsilon_y$  is the model uncertainty for geometry function,
- $\varepsilon_{s2}$  is the model uncertainty for stress range calculation,
- $A, B$  are the Weibull stress range parameters.

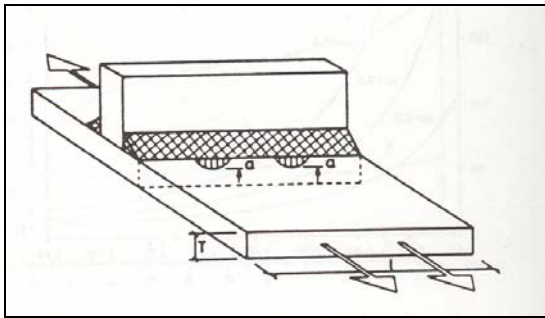


Figure 7 – Illustration of Cracks at Weld Toe

**Cases Studied**

Two different sizes of initial crack depth are considered with a constant aspect ratio 1/20:

- Small Initial Crack – crack depth less than 0.3mm with 95% probability.
- Large Initial Crack – crack depth less than 1.5mm with 95% probability.

In addition to different initial crack sizes, two types of crack growth parameters are considered, with the first type corresponds to the air environment (used within voids or non-water-wetted surfaces), while the second type corresponds to the marine environment with cathodic protection at -850 mV [7]. Table 5 summarizes the cases considered.

**Table 5 – Sensitivity Cases for Fatigue Reliability Variations**

	Small Initial Crack	Large Initial Crack
Air Environment	Case 1	Case 2
Marine Environment	Case 3	Case 4

Figure 8 shows the time-variant fatigue reliabilities of the example connection for the four sensitivity cases. The results show Case 3 drops more from Case 1 than Case 2 drops from Case 1. In other words, the crack growth parameters for different environment appear to have a larger impact on the fatigue reliability than the size of the initial crack.

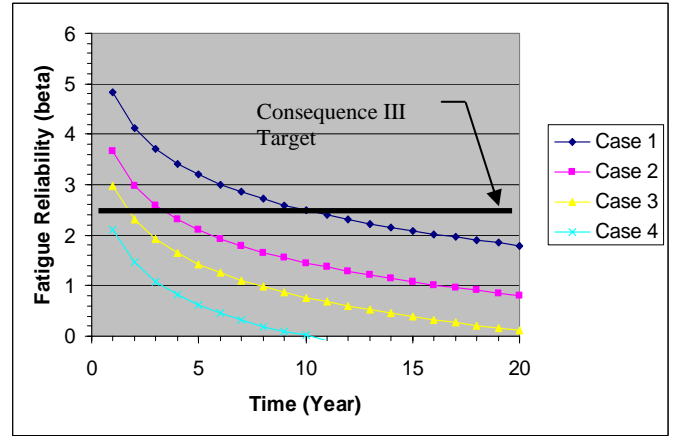


Figure 8 – Lifetime Fatigue Reliability Variations for Sensitivity Cases Studied

**Sensitivity on Inspection Updating**

The probability of fatigue failure at year  $t$ , with inspection performed at year  $t_{inspect}$  ( $t \geq t_{inspect}$ ) is calculated by the following conditional probability equations:

$$P[M_i(t) < 0 | I_{no,i}(t_{inspect}) > 0] \quad (3)$$

for the ‘no cracks found’ scenario, and

$$P[M_i(t) < 0 | I_{yes,i}(t_{inspect}) = 0] \quad (4)$$

for the ‘crack found and measured’ scenario.

The probability of detection used in this study was adopted from the information contained in [6]. These detection probabilities for the close visual and the MPI inspection are shown in Figure 9. With reference to this figure, the probability of detection (POD) can be represented by the following Exponential distribution:

$$F(x) = 1 - \exp(-\lambda \cdot (x - \tau)) \quad (5)$$

The distribution parameters for the close visual and the MPI inspections can be found in [1].

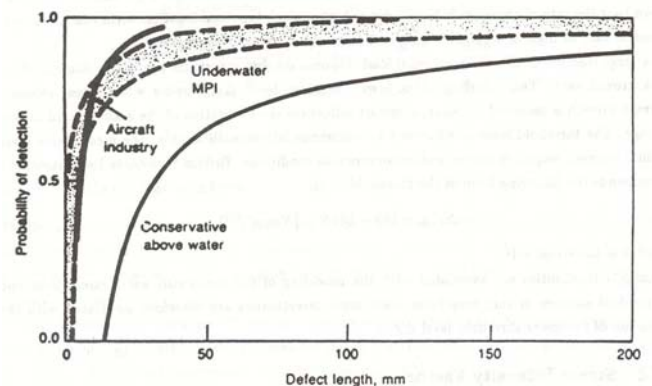
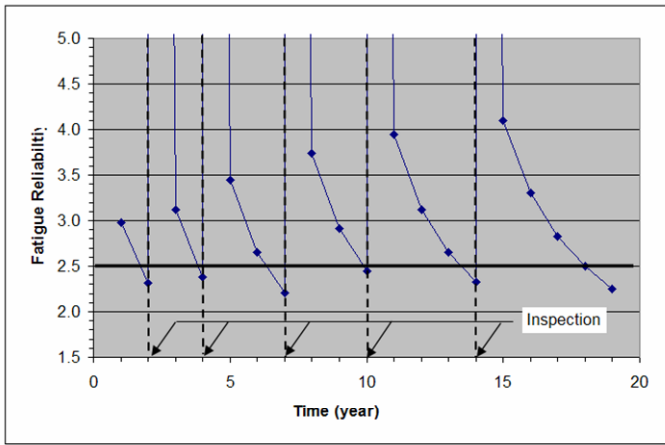


Figure 9 - Probability of Detection for the Close Visual Inspection and MPI Inspection [6]

The fatigue reliability updating for all four sensitivity cases were carried out using the formulations as presented above and assuming the inspection has an accuracy equivalent to the MPI inspection. Furthermore, it is assumed that no cracks were found in all inspections.

Figure 10 shows the results for Case 3, in which inspections were carried out immediately after the time when the fatigue reliability is predicted to fall below the acceptable level. In the Case 3 example, inspections need to be carried out at the 2<sup>nd</sup>, 4<sup>th</sup>, 7<sup>th</sup>, 10<sup>th</sup>, 14<sup>th</sup> and the 18<sup>th</sup> year. It is seen from Figure 10 that once inspections are carried out without finding any cracks, the fatigue reliability index increases dramatically right after the inspection, and then decreases as time elapses.



**Figure 10 – Effects of Inspection Updating for Case 3 Crack**

The time instances when inspections need to be carried out are summarized in Table 6 for all sensitivity cases. In this Table, the years necessary for inspections as predicted from fatigue reliability analysis are marked.

It is observed from Table 6 that once inspections are carried out without finding cracks, the effects of assumed initial crack sizes are greatly diminished. For example, after the 1<sup>st</sup> inspection for Cases 1 and 2, although occurring at different time instances, the next inspection cycles follow a seven to eight years frequency for both cases. A similar phenomenon applies to the comparison between Cases 3 and 4.

**Table 6 – Example Inspection Interval for Sensitivity Case Studies**

	Year for Inspection																			
	1	2	3	4	5	6	7	8	9	10	11	12	13	14	15	16	17	18	19	20
Case 1																				
Case 2																				
Case 3																				
Case 4																				

Table 6 also indicates that for connections subjected to the Marine Environment, more frequent inspections are required compared to connections exposed to the Air Environment. The increased frequency for the Marine Environment connections is approximately two to three times more compared to the Air Environment connections.

Although from Table 6 it is predicted that Cases 3 and 4 need to be inspected on a three to four year cycle, it is important to point out that inspections can be rotated among a group of similar connections such that between every three to four years the inspections do not have to be done on the same set of connections. Correlations between a large sample of connections can be utilized such that only a percentage of total connections are inspected during the first inspection. If the inspection shows favorable results then by way of statistical correlation the remaining number of connections will have sufficient fatigue reliability. For the next inspection three to four years later, a second group of similar connections are then inspected.

Based on these considerations mentioned above, the more unfavorable Marine Environment does not necessarily result in a significant increase in inspection cost. By intelligently grouping the connections and rotating the inspection schedule among them, high fatigue reliability for these connections can still be maintained.

**Conclusion**

The conclusions found from this study can be summarized as follows:

- Corrosion rates have a higher impact on strength reliability than environmental load conditions when considering the strength driven degradation (corrosion causing either yielding or buckling).
- High probabilistic corrosion rates show a very unfavorable trend to precipitate the reliability curve while the harsh environmental load shows a more favorable trend of maintaining the same slope as other more benign environmental conditions.
- High strength reliability for the harsh environmental load conditions can be achieved by reducing corrosion rates, which in turn can be achieved by
  - Implementing corrosion control measure to reduce the expected corrosion rates, and/or
  - Closely monitoring corrosion rate to reduce their uncertainty.
- The crack growth parameters between the Air Environment and Marine Environment (with the same initial crack size) have a larger impact on different initial crack sizes (with the same crack growth parameters).
- From fatigue reliability updating analysis, assumed initial crack sizes have little effect on subsequent inspection schedule once the first inspection is conducted.
- The subsequent inspection schedule (after the 1<sup>st</sup> inspection) for the Marine Environment exposed connections needs to be two to three times more frequent than the Air Environment connections.
- When statistical correlations among like connections (addressed in a companion paper, [1]) are considered, rotation of inspections on sub-groups for each scheduled inspections can reduce inspection cost while still maintaining necessary fatigue reliability.

**Acknowledgements**

The authors wish to thank their respective companies for the opportunity to publish this paper.

---

**References**

1. Ku, A., Serratella, C., Spong, R., Basu, R., Wang, G., Angevine, D., Structural Reliability Applications in Developing Risk-Based Inspection Plans for a Floating Production Installation, *Proceedings of the Offshore Mechanics and Arctic Engineering Conference*, OMAE2004-51119, Vancouver, 2004.
2. Ship Structure Committee, *Probability Based Ship Design: Implementation of Design Guidelines*, SSC-392, 1996.
3. American Bureau of Shipping, *Rules for Building and Classing Steel Vessels*, 2004.
4. Xu, L., Nick, C. and Shin, Y., Implementation of Hindcast Global Wave Data for Design and Analysis of Marine Structures, *Deep Offshore Technology*, 2000.
5. Wang, G. and Spong, R., Experience Based Data for FPSO's Structural Design, *Proceedings of the Offshore Technology Conference*, OTC 15068, 2003.
6. Ship Structure Committee, *Ship Maintenance Project: Fatigue Damage Evaluation*, SSC-386-I, 1995.
7. BSI, *Guide on Methods for Assessing the Acceptability of Flaws in Metallic Structures*, BS 7910:1999.
8. TSCF (1997). *Guidance Manual for Tanker Structures*, Tanker Structure Co-operative Forum, Witherby & Co. Ltd.